HHS Public Access

Author manuscript

Nature. Author manuscript; available in PMC 2012 September 15.

Published in final edited form as:

Nature. ; 483(7389): 345–349. doi:10.1038/nature10863.

Goblet cells deliver luminal antigen to CD103+ DCs in the small intestine

Jeremiah R. McDole[1,*], **Leroy W. Wheeler**[2,*], **Keely G. McDonald**[2], **Baomei Wang**[1], **Vjollca Konjufca**[3], **Kathryn A. Knoop**[2], **Rodney D. Newberry**[2,*], and **Mark J. Miller**[1,*]

[1]Department of Pathology and Immunology, Washington University School of Medicine, St. Louis, MO 63110, USA

[2]Department of Internal Medicine, Washington University School of Medicine, St. Louis, MO 63110, USA

[3]Department of Microbiology, Southern Illinois University, Carbondale, IL 62901

Abstract

The intestinal immune system is exposed to a mixture of foreign antigens from diet, commensal flora, and potential pathogens. Understanding how pathogen-specific immunity is elicited while avoiding inappropriate responses to the background of innocuous antigens is essential for understanding and treating intestinal infections and inflammatory diseases. The ingestion of protein antigen can induce oral tolerance, which is mediated in part by a subset of intestinal dendritic cells (DCs) that promote the development of regulatory T cells[1]. The lamina propria (LP) underlies the expansive single cell absorptive villous epithelium and contains a large population of DCs ($CD11c^+$ $CD11b^+$ $MHCII^+$ cells) comprised of two predominant subsets; $CD103^+$ CX_3CR1^- DCs, which promote IgA production, imprint gut homing on lymphocytes, and induce the development of regulatory T cells[2–9], and $CD103^-$ CX_3CR1^+ DCs (with features of macrophages), which promote TNFα production, colitis, and the development of Th17 T cells[5–7,10]. However the mechanisms by which different intestinal LP-DC subsets capture luminal antigens *in vivo* remains largely unexplored. Using a minimally disruptive *in vivo* imaging approach we show that in the steady-state, small intestine goblet cells (GCs) function as passages delivering low molecular weight soluble antigens from the intestinal lumen to underlying $CD103^+$ LP-DCs. The preferential delivery of antigens to DCs with tolerogenic properties implies a key role for this GC function in intestinal immune homeostasis.

Correspondence: Mark J. Miller miller@pathology.wustl.edu Phone: 314 362 3044 Fax: 314 362 4096. Rodney D. Newberry rnewberry@wustl.edu Phone: 314 362 2671 Fax: 314 362 2609.

*These authors contributed equally to the work

Supplementary information is linked to the online version of the manuscript

Author Contributions: J.R.M., B.W., and V.K. performed 2P imaging experiments and data analysis, L.W.W., K.A.K., and K.G.M. performed cell isolation, *in vitro* studies, and immunofluorescence and data analysis, R.D.N. and M.J.M conceived of the study, directed the experimental design, analyzed the data, and wrote the manuscript. J.R.M and L.W.W. contributed equally to this work. All authors reviewed and discussed the manuscript.

We examined the *in vivo* antigen acquisition behavior of intestinal LP-DCs in fluorescent DC-reporter mice using two-photon (2P) microscopy (Supplementary Fig. 1a). The intestine is imaged within the peritoneal cavity and images can be acquired from either the intact intestinal serosa or from luminal surface through a small longitudinal incision in the intestine (Fig. 1a, b and Supplementary Movie 1). The preparation is sufficiently stable to permit 3D imaging of DC behavior deep within intestinal tissues (Fig. 1c and Supplementary Movie 1) and preserves blood flow and epithelial barrier integrity for greater than 4hrs of continuous imaging.

We assessed antigen distribution by 2P microscopy following the intraluminal injection of 10kD rhodamine dextran as a model antigen. Dextran coated the surface of the epithelium and filled the space between villi and the crypts (Fig. 1a, b). In addition, we observed cylindrical dextran columns ~5μm in diameter and ~20μm long projecting through the villus epithelium and into the LP, when imaging from either serosal or luminal orientations (Fig. 1a–c, Supplementary Fig.1b, and Supplementary Movie 1). Trans-epithelial dextran columns were common throughout the small intestine from duodenum to ileum, but did not cause a general disruption of the epithelial barrier as shown by the exclusion of dextran from the LP (Fig. 1a–c). We did not detect trans-epithelial dextran columns in the stomach, cecum, or colon, with the exception of the epithelium overlying the cecal patches (Supplementary Fig. 1 c–e; Supplementary Movie 2). Confocal microscopy reveled that dextran columns were a subset of epithelial cells containing intracellular dextran, which had a continuous border of e-cadherin on their basolateral surface and were often in contact with CD11c-YFP^{+} LP-DCs (Fig 1 d and e).

Periodic acid-Schiff (PAS) staining of mucin in sections of small intestine (Fig. 2a) produced a goblet cell (GC) staining pattern similar in frequency, distribution, and dimensions to the dextran columns identified by 2P microscopy (Fig. 2b and c). Furthermore, in contrast to the acellular and impermeable discontinuities seen in the small intestine epithelium[11], dextran columns were associated with a nucleus (Fig. 2d; Supplementary Fig. 2a; Supplementary Movie 3). To determine if the dextran filled cells were in fact GCs, sections of intestine from mice given lysine-fixable dextran were stained with antibodies to mucin 2 (MUC2) and cytokeratin 18, which are both highly expressed by GCs[12]. Dextran columns , showed near prefect co-localization with MUC2^{+} and cytokeratin 18^{+} epithelial cells displaying GC morphology (Fig. 2e, f). Therefore, we term this phenomenon “goblet cell-associated antigen passages” (GAPs). To address the possibility that GAPs are apoptotic GCs, we co-stained for various markers of apoptosis including cleaved cytokeratin 18, cleaved caspase 3, and TUNEL (Supplementary Fig 3 a–i). In all cases, we found no association between apoptotic GCs and GAPs. Moreover, GAPs are distinct from villous M-cells, since they did not co-localize with the M-cell marker glycoprotein 2 (GP2) (Fig. 2g)[13]. The frequency and distribution of GAPs assessed by 2P microscopy was similar in all strains of specific-pathogen-free (SPF) mice examined (supplementary Fig. 2 b–d), with a non-significant trend more GAPs detected in the terminal ileum (supplementary Fig. 2h). GAPS were also evident in human jejunum resection specimens (Fig. 2h, i), suggesting that GAPs are a general phenomenon of the healthy small intestine. We examined the frequency of GAPs in C3H/HejBir IL-10$^{-/-}$ mice[14], which

develop spontaneous intestinal inflammation with GC loss, and in germ-free (GF) mice that lack normal gut flora. The number of GAPs and GCs correlated strongly; GAPs and GCs were significantly more numerous in GF mice (supplementary Fig. 2 e and g) and significantly fewer in IL-10$^{-/-}$ mice (supplementary Fig. 2 f and g).

Previous studies have shown that LP-DCs can extend trans-epithelial dendrites (TEDs) between intestinal epithelial cells to sample luminal contents and microbiota[15–18]. However, these studies employed *ex vivo* and exteriorized tissue preparations that involved removing the luminal contents and mucous before imaging. Using our *in vivo* imaging preparation, we found that although LP-DCs probed the epithelium actively with their dendrites (Fig. 1c; Supplementary Movie 1), they did not extend TEDs into the intestinal lumen to capture fluorescent antigen in healthy mice (based on over 50 independent intravital imaging experiments examining all regions of the small intestine from the tip of the villi to the base of the crypts). To confirm that our imaging approach can readily detect TEDs, we imaged LP-DC in CD11c^{YFP+} reporter mice challenged mice infected with *Salmonella typhimurium*, which have been shown to upregulate TED formation[15]. Although rare LP-DC TEDs were observed in ~2% of villi, TEDs did not mediate the uptake of luminal dextran or beads based on fluorescence co-localization (Supplementary Fig. 4a; Supplementary Movie 4).

Next, we examined whether paracellular leak[19] could serve as a major source of luminal antigen for small intestine LP-DCs. The intraluminal injection of 5mg of 10kD dextran, produced a faint “feather” like staining pattern between villous epithelial cells, consistent with paracellular leak (Supplementary Fig. 4b, Supplementary Movie 4). Time-lapse 2P imaging showed that dextran collected at the base of the epithelium, but was flushed out of the villi efficiently during contraction and did not remain co-localized with LP-DCs even in areas of extensive paracellular leak (Supplementary Fig. 4b, Supplementary Movie 4). In addition, we did not detect paracellular leak around GAPs in fixed sections by confocal microscopy, despite the more permissive tight junctions of GCs[20]. However, we cannot exclude the possibility that LP-DCs capture low levels of antigen via paracellular leak, since this process might be below the level of detection of our imaging approach.

In contrast to TEDs and paracellular leak, 2P time-lapse imaging provided direct evidence that GAPs are a source of luminal antigen for LP-DCs. In addition to dextran (Fig. 3a), GAPs were capable of transporting protein antigens (Fig. 3b). Although most GAPs remained visible for the duration of our imaging experiments, they were a dynamic phenomenon (Supplementary Movie 5 lower panels). Moreover, the manner in which LP-DCs interacted with GAPs varied. In some cases, DCs made stable contacts and slowly collected antigen over several minutes (Fig. 3a, Supplementary Movie 5 lower left panel) while in others, DCs actively probed GAPs and captured clumps of antigen (Fig. 3b; Supplementary Movie 5 lower right panel). We assessed the molecular weight exclusion limit of GAPs and found that beads ranging from 0.02–1.0μm in size did not enter GAPs (Supplementary Fig. 4c). In contrast, GAPs filled rapidly with 10kD dextran (Supplementary Fig. 4d) and dextran co-localized with CD11c^{YFP+} LP-DCs 2hrs after intraluminal injection (Fig. 3a and Supplemental movie 4 lower left panel). GAPs also filled with larger dextrans (Supplementary Fig. 4d), however capture by LP-DCs was markedly

reduced with 70kD dextran and undetectable with 2,000kD dextran during our 4hrs imaging window.

The small intestine LP contains two prominent DC populations: CX_3CR1^{-}, $CD103^{+}$ DCs with tolerogenic potential, and CX_3CR1^{+}, $CD103^{-}$ DCs that have features of macrophages and have been implicated in intestinal inflammation[5–10]. We visualized LP DC subsets *in vivo* using dual reporter $CD11c^{YFP}$ CX_3CR1^{GFP} mice in which $CD103^{-}$ and $CD103^{+}$ LP-DCs can be distinguished by the presence or absence of CX_3CR1^{GFP} expression respectively (Fig. 3c; Supplementary Fig. 5). We frequently observed $CD11c^{YFP+}$ CX_3CR1^{GFP} LP-DCs sampling GAPs by 2P microscopy, but this behavior was rare in $CD11c^{YFP+}$ CX_3CR1^{GFP+} LP-DCs (Fig. 3c); out of 50 total LP-DCs containing dextran, 49 were $CD11c^{YFP+}$ CX_3CR1^{GFP-}. Furthermore, when we directly observed antigen transfer from GAPs to DCs (20 out of 500 GAPs examined), GAPs delivered antigen exclusively to $CD11c^{YFP+}$ CX_3CR1^{GFP-} LP-DCs (Fig. 3d). Immunofluorescence microscopy confirmed that the cells interacting with GCs were $CD103^{+}$ $CD11c^{+}$ LP-DCs and not $B220^{+}$ plasmacytoid DCs (pDCs) (Supplementary Fig 6a). Moreover, flow cytometry revealed that luminal antigen was captured preferentially by $CD103^{+}$ DCs at a proportion of roughly 10:1 over $CD103^{-}$ DCs (Fig. 3e) and rarely colocalized with pDCs (Supplementary figure 6b), consistent with the sampling bias observed by 2P imaging. Control experiments demonstrated that antigen uptake during cell isolation was negligible (Supplementary Fig. 7), thus the flow cytometry results measure the *in vivo* antigen acquisition capacity of different LP-DC subsets. Interestingly, $CD103^{+}$ LP-DCs, but not $CD103^{-}$ LP-DCs, often stained positive for cytokeratin 18 (Fig. 3f and g), which is highly expressed by villous GCs (Fig. 3h). Since cytokeratin 18 expression is undetectable in LP-DCs by quantitative real time PCR (Fig. 3h), this suggests that $CD103^{+}$ LP-DCs interact selectively with GAPs and can capture GC derived proteins.

In 2P imaging experiments, LP-DCs captured fluorescent luminal ovalbumin (Ova) readily from GAPs (Fig. 4a; Supplementary Movie 6), similar to fluorescent dextran and BSA. To determine if LP-DCs could process and present luminal antigen, we administered Ova *in vivo*, then sorted LP-DCs and co-cultured them with OTI T cells[21]. T cell proliferation was assessed on day 3 by both CFDA dilution (Fig. 4b and c) and by counting T cells after culture (Fig. 4d). Total LP-DC populations ($CD45^{+}$, $CD11c^{+}$, $MHCII^{+}$) were capable of inducing modest OTI T cell proliferation that was significantly greater than controls (Fig 4b and d). $CD103^{+}$ LP-DCs stimulated significant OTI T cell proliferation, while $CD103^{-}$ LP-DCs from the same mice did not (Fig. 4d). The failure of $CD103^{-}$ LP-DCs to stimulate T cells was not due a lack of intrinsic antigen presentation capacity, since they were capable of inducing comparable levels of OTI T cell proliferation to $CD103^{+}$ LP-DCs (81.4% to 88.2% respectively) when Ova was added to the cell culture (Fig. 4c). These findings suggest that $CD103^{+}$ LP-DCs have cross-presentation capacity, similar to their mesenteric lymph node conterparts[2].

In some 2P time-lapse recordings we observed of GAPs forming or disappearing (Supplementary movies 3 and 5 lower panels), suggesting that GAP formation could be related to changes in GC function or secretion. To test whether GC secretion was associated with GAP formation, we administered the cholinergic agonist carbamylcholine (CCh) to

stimulate GC secretion and imagined the small intestine with 2P microscopy. Following CCh administration, the frequency of GAPs increased dramatically as did the amount of luminal antigen co-localized with LP-DCs (Fig. 4e and f), while paracellular leak or TEDs were unaffected during our imaging time-frame (Fig. 4f). Furthermore, LPDCs, $CD103^+$ LP-DCs, and $CD103^-$ LP-DCs from CCh treated mice had significantly enhanced the luminal antigen presentation in *ex vivo* T cell proliferation assays (Fig. 4g and Supplementary Fig. 8), indicating that GC secretion is linked mechanistically to GAP formation and luminal antigen delivery.

We also examined whether the increased number of GAPs in GF mice (Fig. 4h and Supplementary figure 2) correlated with increased luminal antigen presentation by LP-DCs. LP-DCs from GF mice given luminal Ova showed significantly increased antigen presentation capacity as compared LP-DCs from SPF mice. Moreover, luminal antigen delivery in GF mice appeared to favor $CD103^+$ LP-DCs over $CD103^-$ LP-DCs (Fig. 4i) similar to observations in SPF mice.

To directly test whether GAPs are a major pathway of antigen delivery to LPDCs, we generated mice with epithelial cell specific deletion in mouse atonal homolog 1 (Math1), a transcription factor required for the development of secretory cell lineages including GCs[22]. $Math1^{fl/flVilCre}$ mice (M1KO) lacked small intestine GCs (Supplementary figure 9 a, b, and c) and *in vivo* 2P imaging revealed a concomitant loss of GAPs, with the epithelium forming a tight barrier to luminal dextran (Fig 4j and Supplementary figure 9d). Moreover, LP-DC populations isolated from M1KO mice given luminal Ova failed to stimulate OTI T cells above background (Figure 4k and supplementary figure 9e). The lack of antigen presentation by $CD103^+$ LP-DCs from M1KO mice was not due to an intrinsic defect, since these LP-DCs were capable of inducing robust T cell proliferation when exogenous Ova was added to the T cell cultures (Supplementary figure 9f). Taken together, these findings suggest that GAPs are a major mechanism for delivering luminal antigens to LP-DCs in the steady-state.

Understanding how the balance between tolerance and immunity is achieved at the intestinal mucosa is crucial for oral vaccine development and the treatment of chronic intestinal inflammatory diseases. This study identifies GAPs as a mechanism by which $CD103^+$ LP-DCs can acquire innocuous antigens from the intestinal lumen in the steady-state. How preferential antigen delivery is achieved, is the focus of ongoing studies. Biased delivery could be a natural consequence of $CD103^+$ LP-DC sampling the epithelium more actively or perhaps being recruited selectively by chemoattractants released by or near GCs. GC deficiency or dysfunction in mice and humans has been linked to the development of intestinal inflammation[23–27]. While this association has been attributed to the loss of mucins and other biologically active GC products, our findings suggest that GCs could play a key role in promoting intestinal immune homeostasis by delivering luminal antigen to tolerogenic LP-DCs.

Methods Summary

Mice and human specimens

All mice were on a C57BL/6 background unless otherwise specified. Healthy human jejunal sections were obtained from bariatric surgeries, placed in ice cold PBS and used immediately for imaging. Procedures and protocols were carried out in accordance with the institutional review board at Washington University School of Medicine.

2P microscopy

The intravital imaging preparation used in this study is similar to previously described methods[11,15] with the following differences: imaging is performed with the tissue within the peritoneal cavity, fecal material is not scraped from the mucosal surface and in some experiments atropine (1 mg/kg) was injected subcutaneously to dampen peristaltic movement of the small intestine. At this dose atropine, did not affect the formation of TEDs or GAPs. Model fluorescent antigens, dextran (2–5mg), ovalbumin (2mg), BSA, (2mg) and FluoSpheres (1ml undiluted) (all from Invtirogen, Carlsbad, CA) were injected into the intestinal lumen ~2hrs minutes prior to imaging. Human resection specimens were incubated in 10ug/ml of dextran at room temperature for 1hr prior to imaging.

Methods

Mice and human specimens

C57BL/6 mice, Rag−/− mice, Balb/c mice, IL-10−/− knockout mice on the C3H/HejBir.129 background[14], OTI T cell receptor transgenic mice[21], CX_3CR1^{GFP} knock-in mice[28], $Math1^{fl/fl}$ mice[22], and Villin Cre transgenic mice[29], were purchased from The Jackson Laboratory (Bar Harbor, MN). $CD11c^{YFP}$ transgenic mice[30] were a gift from Michel Nussenzweig (The Rockefeller University, New York, NY) and LysM-GFP mice[31] were a gift of Klaus Ley (LIAI, La Jolla, CA). Gnotobiotic mice were obtained from the Washington University Digestive Disease Research Core Center murine models core. Animals, other than gnotobiotic mice, were housed in a specific pathogen free facility and fed routine chow diet. Animals were 8 to 16 weeks of age at the time of analysis. Intestines from mice receiving 250 rads of gamma irradiation and sacrificed 6 hours later served a positive control for apoptosis markers. All mice were on a C57BL/6 background unless otherwise specified. Healthy human jejunal sections were obtained from bariatric surgeries, placed in ice cold PBS and used immediately for imaging. Procedures and protocols were carried out in accordance with the institutional review board at Washington University School of Medicine.

Intravital 2P microscopy

The intravital imaging preparation used in this study is similar to previously described methods[11,15] with the following differences: the intestine is not exteriorized during imaging, fecal material is not scraped from the mucosal surface and in some experiments atropine (1 mg/kg) was injected subcutaneously to dampen peristaltic movement of the small intestine. Mice were anesthetized with isofluorane and a small vertical incision was made in the abdominal wall to expose the peritoneal cavity and contents. The intestine is secured to the

bottom of a glass coverslip on the upper chamber plate using a thin ring of Vetbond tissue adhesive (3M). Because the coverslip sits directly over the incision in the mouse's abdomen the tissue remains in the peritoneal cavity for imaging. No additional manipulations were performed to image from the serosal surface. The imaging chamber was maintained at 37°C using a dual-channel heating system (Warner Instruments). To image from the luminal surface, a small longitudinal incision was made in the intestine taking care to avoid large blood vessels. Model fluorescent antigens, dextran (2–5mg), ovalbumin (2mg), BSA, (2mg) and FluoSpheres (1ml undiluted) (all from Invtirogen, Carlsbad, CA) were injected into the intestinal lumen ~2hrs prior to imaging. Human resection specimens were incubated in 10ug/ml of dextran at room temperature for 1hr prior to imaging. Time-lapse imaging was performed with a custom built 2P microscope running ImageWarp acquisition software (A&B Software, New London, CT). For time-lapse imaging, we averaged 15 video-rate frames (0.5 sec per slice) during the acquisition. Each plane represents an image of 220 × 240 um in the x and y dimensions. 21 to 31 sequential z-steps (2.5 μm each) were acquired to form a z-stack. In our experiments epithelial integrity was assessed by dextran and DAPI staining, which in healthy tissue, demarcates the luminal surface of the epithelium (aside from GAPs) and shows an ordered arrangement of DAPI stained nuclei respectively. In some experiments mice were given 10^8 *Salmonella typhimurium* strain χ3716 orally 24–72 hours prior to imaging.

Flow cytometry, immunohistochemistry, and confocal microscopy

Flow cytometry and the staining of intestine sections was performed as previously described[32]. Reagents used for flow cytometry include, anti-CD11c, anti-CD45, anti-CD4, anti-MHCII, anti-CD3, anti-CD8a, anti-PDCA-1 (all from eBioscience, SanDiego, CA), 7-AAD, anti-CD103, and anti-B220 (both from BDBiosciences, SanDiego, CA). Data was acquired with a FACScan cytometer (BD Biosciences, San Jose, CA) retrofitted with additional lasers. Data acquisition was performed using CellQuest (BD Biosciences) and Rainbow (Cytek, Fremont, CA) or FlowJo software (Tree Star, Ashland, OR). Data analysis was performed on a Macintosh computer running FlowJo software.

To immobilize the lysine fixable fluorescent dextrans, intestinal sections were treated with 2% paraformaldehye immediately after 2P imaging. Reagents used for immunhistochemistry include 4',6-diamidino-2-phenylindole (DAPI; SigmaAldrich, St. Louis, MO), anti-CD11c, anti-CD103, anti-e cadherin (all from BDBiosciences), anti-cytokeratin 18 and anti-muc2 (both from abcam, San Francisco, CA), anti-GP2 (MBL International, Woburn, MA), anti-cleaved cytokeratin 18 (Enzo Life Sciences, Farmingdale, NY), and anti-cleaved caspase 3 (Cell Signaling Technology, Boston, MA). The Terminal deoxynucleotidyl transferase-mediated dUTP nick end labeling (TUNEL) assay (Trevigen, Gaithersburg, MD) was performed per the manufacturers recommendations. Confocal microscopy was performed using a Zeiss LSM510 Meta laser scanning confocal microscope (Carl Zeiss, Inc., Thornwood, NY) equipped with a 63×, 1.4 numerical aperature Zeiss Plan Apochromat oil objective. Images were obtained using the Zeiss LSM510 software.

T-cell proliferation assays

Mice were anesthetized and the small intestine injected intraluminally with 2mg of ovalbumin (SigmaAldrich) dissolved in phosphate buffered saline (PBS), or PBS alone (controls) as in the 2P imaging experiments. In some experiments mice received 3μg of carbamylcholine (SigmaAldrich) subcutaneously twenty minutes after the administration of luminal ovalbumin. Two hours after the administration of ovalbumin, cell populations were isolated from the intestinal lamina propria as previously described[32] and sorted by flow cytometry into total LP-DC populations (CD45+ MHCII+ CD11c+), CD103+ DC populations (CD45+ MHCII+ CD11c+ CD103+), or CD103− DC populations (CD45+ MHCII+ CD11c+ CD103−). Sorted DC populations were cultured with sorted CFDA (Invitrogen, Grand Island, NY) labeled OTI splenic T cells at a ratio of 1:10 DC to T cells. As a positive control, 20μg of Ova was added to cultures of DC populations isolated from mice receiving luminal PBS, unless otherwise stated. After 3 days cultures were evaluated for CFDA dilution and the number of T cells by flow cytometry and cell counting.

Real time PCR

RNA isolation, cDNA synthesis, standard curve construction, and real time PCR was performed as previously described[32]. The following primers were used: 18s, forward, 5'-CGG CTA CCA CAT CCA AGG AA-3', and reverse, 5'-GCT GGA ATT ACC GCG GCT-3'□; cytokeratin 18, forward, 5'-CAG CCA GCG TCT ATG CAG G-3', and reverse, 5'-CTT TCT CGG TCT GGA TTC CAC-3'. Small intestine epithelial cell populations were stained with cytokeratin 18 and AlexaFluor 488 (Invitrogen) labeled lectin from *Ulex europaeus* (UEA-I; Sigma-Aldrich). Goblet cell populations were isolated by flow cytometric sorting as UEA-I+ cytokeratin 18+ cells.

Statistical Analysis

Data analysis using a and Student's *t* test or a one way ANOVA with a Tukey's post test were performed using GraphPad Prism (GraphPad Software Inc., San Diego, CA).

Supplementary Material

Refer to Web version on PubMed Central for supplementary material.

Acknowledgements

This work was supported in part by grants DK064798 (RDN), AI083538 (RDN), AI095550 (RDN and MJM), DK085941 (LWW), and AI077600 (MJM). The authors thank Wandy Beatty for assistance with confocal microscopy, Christopher Eagon for assistance with human specimens, the Alvin J. Siteman Cancer Center at Washington University School of Medicine and Barnes-Jewish Hospital in St. Louis, Mo., for the use of the Siteman Flow Cytometry Core, which provided high speed flow sorting and the Washington University Digestive Disease Research Core Center (DDRCC), which provided gnotobiotic mice. The Siteman Cancer Center is supported in part by an NCI Cancer Center Support Grant #P30 CA91842. The Washington University DDRCC is supported by grant P30-DK52574.

References

1. Weiner HL, da Cunha AP, Quintana F, Wu H. Oral tolerance. Immunol Rev. 241:241–259. doi: 10.1111/j.1600-065×.2011.01017.x. [PubMed: 21488901]

2. Jaensson E, et al. Small intestinal CD103+ dendritic cells display unique functional properties that are conserved between mice and humans. J Exp Med. 2008; 205:2139–2149. doi:10.1084/jem.20080414. [PubMed: 18710932]

3. Johansson-Lindbom B. Functional specialization of gut CD103+ dendritic cells in the regulation of tissue-selective T cell homing. J Exp Med. 2005; 202:1063–1073. doi:10.1084/jem.20051100. [PubMed: 16216890]

4. Uematsu S, et al. Regulation of humoral and cellular gut immunity by lamina propria dendritic cells expressing Toll-like receptor 5. Nat Immunol. 2008; 9:769–776. doi:10.1038/ni.1622. [PubMed: 18516037]

5. Varol C, et al. Intestinal Lamina Propria Dendritic Cell Subsets Have Different Origin and Functions. Immunity. 2009; 31:502–512. doi:10.1016/j.immuni.2009.06.025. [PubMed: 19733097]

6. Schulz O, et al. Intestinal CD103+, but not CX3CR1+, antigen sampling cells migrate in lymph and serve classical dendritic cell functions. J Exp Med. 2009; 206:3101–3114. doi:10.1084/jem.20091925. [PubMed: 20008524]

7. Bogunovic M, et al. Origin of the lamina propria dendritic cell network. Immunity. 2009; 31:513–525. doi:10.1016/j.immuni.2009.08.010. [PubMed: 19733489]

8. Coombes JL, et al. A functionally specialized population of mucosal CD103+ DCs induces Foxp3+ regulatory T cells via a TGF-beta and retinoic acid-dependent mechanism. J Exp Med. 2007; 204:1757–1764. doi:10.1084/jem.20070590. [PubMed: 17620361]

9. Sun CM, et al. Small intestine lamina propria dendritic cells promote de novo generation of Foxp3 T reg cells via retinoic acid. J Exp Med. 2007; 204:1775–1785. doi:10.1084/jem.20070602. [PubMed: 17620362]

10. Niess JH, Adler G. Enteric Flora Expands Gut Lamina Propria CX3CR1+ Dendritic Cells Supporting Inflammatory Immune Responses under Normal and Inflammatory Conditions. The Journal of Immunology. 2010; 184:2026–2037. doi:10.4049/jimmunol.0901936. [PubMed: 20089703]

11. Watson AJ, et al. Epithelial barrier function in vivo is sustained despite gaps in epithelial layers. Gastroenterology. 2005; 129:902–912. doi:S0016-5085(05)01117-0 [pii] 10. 1053/j.gastro.2005.06.015. [PubMed: 16143130]

12. Hesse M, et al. A mutation of keratin 18 within the coil 1A consensus motif causes widespread keratin aggregation but cell type-restricted lethality in mice. Experimental Cell Research. 2007; 313:3127–3140. doi:10.1016/j.yexcr.2007.05.019. [PubMed: 17617404]

13. Hase K, et al. Uptake through glycoprotein 2 of FimH(+) bacteria by M cells initiates mucosal immune response. Nature. 2009; 462:226–230. doi:10.1038/nature08529. [PubMed: 19907495]

14. Kuhn R, Lohler J, Rennick D, Rajewsky K, Muller W. Interleukin-10-deficient mice develop chronic enterocolitis. Cell. 1993; 75:263–274. doi:0092-8674(93)80068-P [pii]. [PubMed: 8402911]

15. Chieppa M, Rescigno M, Huang AY, Germain RN. Dynamic imaging of dendritic cell extension into the small bowel lumen in response to epithelial cell TLR engagement. J Exp Med. 2006; 203:2841–2852. [PubMed: 17145958]

16. Niess JH. CX3CR1-Mediated Dendritic Cell Access to the Intestinal Lumen and Bacterial Clearance. Science. 2005; 307:254–258. doi:10.1126/science.1102901. [PubMed: 15653504]

17. Rescigno M, et al. Dendritic cells express tight junction proteins and penetrate gut epithelial monolayers to sample bacteria. Nat Immunol. 2001; 2:361–367. doi:10.1038/86373. [PubMed: 11276208]

18. Rescigno M, Rotta G, Valzasina B, Ricciardi-Castagnoli P. Dendritic cells shuttle microbes across gut epithelial monolayers. Immunobiology. 2001; 204:572–581. [PubMed: 11846220]

19. Shen L, Weber CR, Raleigh DR, Yu D, Turner JR. Tight Junction Pore and Leak Pathways: A Dynamic Duo. Annual Review of Physiology. 2011; 73:283–309. doi:10.1146/annurev-physiol-012110-142150.

20. Madara JL, Trier JS. Structure and permeability of goblet cell tight junctions in rat small intestine. J Membr Biol. 1982; 66:145–157. [PubMed: 7077649]

21. Hogquist KA, et al. T cell receptor antagonist peptides induce positive selection. Cell. 1994; 76:17–27. doi:0092-8674(94)90169-4 [pii]. [PubMed: 8287475]

22. Shroyer NF, et al. Intestine-specific ablation of mouse atonal homolog 1 (Math1) reveals a role in cellular homeostasis. Gastroenterology. 2007; 132:2478–2488. doi:S0016-5085(07)00571-9 [pii] 10 1053/j.gastro.2007.03.047. [PubMed: 17570220]

23. Dvorak AM, Dickersin GR. Crohn's disease: transmission electron microscopic studies. I. Barrier function. Possible changes related to alterations of cell coat, mucous coat, epithelial cells, and Paneth cells. Hum Pathol. 1980; 11:561–571. [PubMed: 7429506]

24. Eri RD, et al. An intestinal epithelial defect conferring ER stress results in inflammation involving both innate and adaptive immunity. Mucosal Immunology. 2010:1–11. doi:10.1038/mi.2010.74.

25. Trabucchi E, et al. Differential diagnosis of Crohn's disease of the colon from ulcerative colitis: ultrastructure study with the scanning electron microscope. Int J Tissue React. 1986; 8:79–84. [PubMed: 3949447]

26. Tytgat KM, van der Wal JW, Einerhand AW, Buller HA, Dekker J. Quantitative analysis of MUC2 synthesis in ulcerative colitis. Biochem Biophys Res Commun. 1996; 224:397–405. doi:10.1006/bbrc.1996.1039. [PubMed: 8702401]

27. Van der Sluis M, et al. Muc2-deficient mice spontaneously develop colitis, indicating that MUC2 is critical for colonic protection. Gastroenterology. 2006; 131:117–129. doi:10.1053/j.gastro.2006.04.020. [PubMed: 16831596]

28. Jung S, et al. Analysis of fractalkine receptor CX(3)CR1 function by targeted deletion and green fluorescent protein reporter gene insertion. Mol Cell Biol. 2000; 20:4106–4114. [PubMed: 10805752]

29. Madison BB, et al. Cis elements of the villin gene control expression in restricted domains of the vertical (crypt) and horizontal (duodenum, cecum) axes of the intestine. J Biol Chem. 2002; 277:33275–33283. doi:10.1074/jbc.M204935200 M204935200 [pii]. [PubMed: 12065599]

30. Lindquist RL, et al. Visualizing dendritic cell networks in vivo. Nat Immunol. 2004; 5:1243–1250. doi:10.1038/ni1139. [PubMed: 15543150]

31. Faust N, Varas F, Kelly LM, Heck S, Graf T. Insertion of enhanced green fluorescent protein into the lysozyme gene creates mice with green fluorescent granulocytes and macrophages. Blood. 2000; 96:719–726. [PubMed: 10887140]

32. McDonald KG, McDonough JS, Dieckgraefe BK, Newberry RD. Dendritic Cells Produce CXCL13 and Participate in the Development of Murine Small Intestine Lymphoid Tissues. Am J Pathol. 2010; 176:2367–2377. doi:10.2353/ajpath.2010.090723. [PubMed: 20304952]

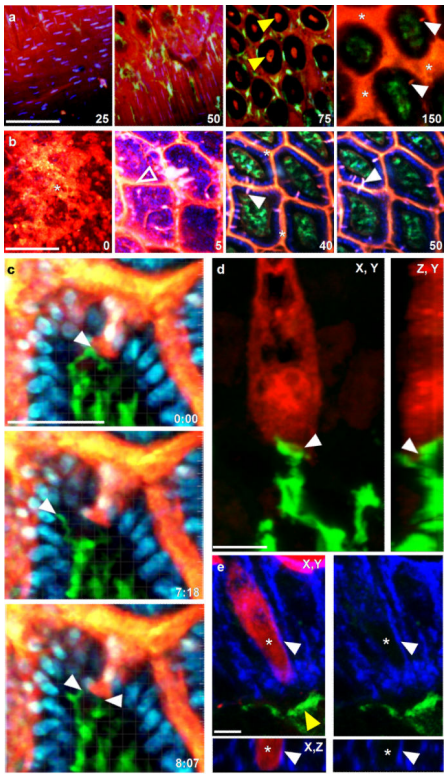

Figure 1. Steady-state trans-epithelial delivery of luminal material in the mouse small intestine

Intestines from CD11c^{YFP} reporter mice injected intraluminally with 10kD dextran (red) imaged with intravital 2P microscopy from the (a) serosal or (b) luminal surfaces. Optical sections at increasing depths (shown in μm) revealed dextran in the lumen (asterisks), the crypts (yellow arrows), on the epithelial surface (unfilled arrow) and columns of dextran that traversed the epithelium (white arrows). Dextran was generally excluded from the LP as identified by CD11c^{YFP+} LP-DCs (green) below the DAPI stained epithelial nuclei (blue in b). Scale bars = 100μm. (c) Time-lapse recording of LP-DC (green) making repeated contacts with a dextran column (red, white arrow) crossing the epithelium (DAPI stained nuclei, blue). Scale bar=50μm, time stamp=min:sec elapsed time from the start of imaging. (d) Rendered confocal image of a CD11c-YFP^{+} DC (green) in contact with a dextran filled epithelial cell (red). Panels show orthogonal views; contact is indicated by the white arrow. Scale bar = 5μm. (e) Confocal image of a dextran containing cell (red) bordered by a continuous e-cadherin (blue) positive surface (white arrow). Asterisk indicates the position of an optical section near the cell's center showing intracellular dextran. A CD11c^{YFP+} DC (green, yellow arrow) positioned near the base of the epithelium. Orthogonal projection (bottom panels); red channel removed (right panels). Scale bar= 5 μm.

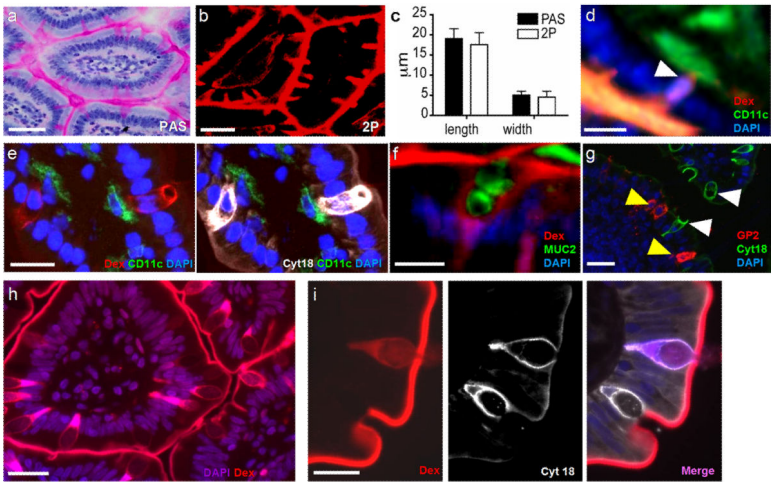

Figure 2. GCs are associated with the trans-epithelial passage of luminal material

(a) PAS staining of GCs and (b) dextran columns visualized by 2P microscopy displayed similar morphology and (c) dimensions. (d) Dextran columns were often associated with a nucleus (white arrow). Dextran columns co-localized with GC markers (e) cytokeratin 18 (cyt18, white) and (f) MUC2. (g) Cytokeratin 18 positive cells (white arrows) did not co-localize with the M-cell marker GP2 (yellow arrows). Dextran columns were present in (h) healthy human small intestine and (i) stained positive for cytokeratin 18. Scale bars = 30μm (a, b, and h), 20 μm (d, e, g, and i), and 10μm (f). Error bars = SD.

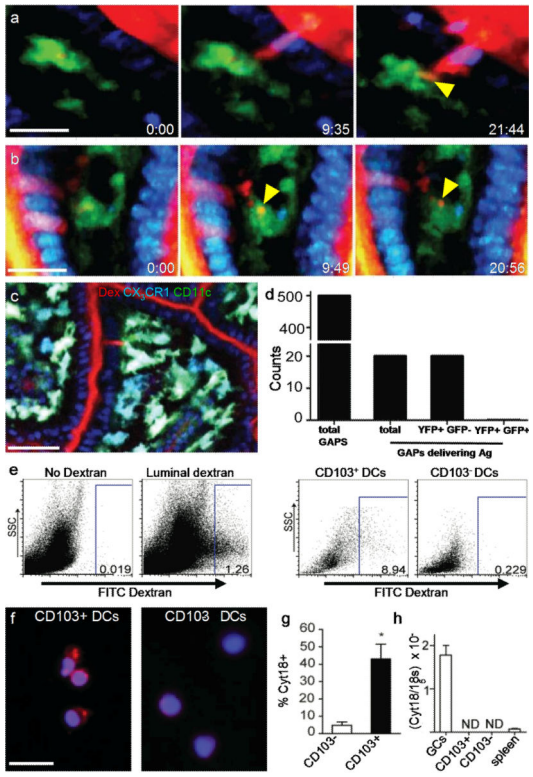

Figure 3. GAPs deliver soluble antigen to CD103$^+$ LP-DCs in the steady-state

Time-lapse 2P imaging of model antigens (red) (a) dextran and (b) bovine serum albumin (BSA) delivered by GAPs to LP-DCs (CD11c^{YFP} = green). Antigen from GAPs co-localized with LP-DCs (yellow arrow) over time). (c) 2P Imaging of CD11c^{YFP} CX3CR1^{GFP} mice. GAPs delivered antigen preferentially to CD103$^+$ LP-DCs (CD11c^{YFP}+ CX_3CR1^{GFP} -; green) over CD103$^-$ LP-DCs (CD11c^{YFP}+ CX3CR1^{GFP}+; cyan) LP-DCs. (d) Enumeration of GAPs and GAPs delivering antigen to LP-DC subtypes in CD11c^{YFP} CX3CR1^{GFP} mice in 2P recordings. (e) Flow cytometry of LP cells revealed that CD103$^+$ DCs captured more luminal dextran than CD103$^-$ DCs. (f) Cytospins on sorted LP-DCs stained with DAPI (blue) and the GC marker cytokeratin 18 (red). (g) Significantly more CD103$^+$ LP-DCs than CD103$^-$ LP-DCs stained cytokeratin 18 positive per high-powered field ($p = <0.001$). (h) Neither DC population expressed detectable cytokeratin 18 mRNA. Scale bar = 15 μm (a and b), 50μm (c), 25μm (f). Data in (g) taken from 9 or more high powered fields (representing >150 cells) Data in (h) performed in triplicate and is representative of two experiments. Error bars = SEM.

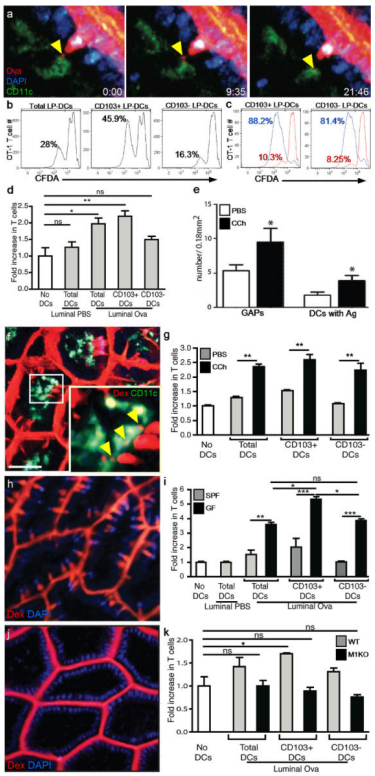

Figure 4. GAPs are a source of luminal antigen for CD103^{+} LP-DCs in the steady-state

(a) 2P time-lapse images of a LP-DC (CD11c^{YFP+}, green) acquiring fluorescent Ova (white arrow) from a GAP (red) in the intestinal epithelium (DAPI stained nuclei, blue). Scale bar = 15 μm; time stamp = min:sec of elapsed time. (b) LP-DC antigen presentation capacity in mice given luminal Ova or PBS assessed on day 3 by (b and c) CFDA dilution and (d) by counting the number of T cells after co-culture with LP-DCs. (c) CD103^{-} LP-DCs induced comparable T cell proliferation to CD103^{+} LP-DCs when exogenous antigen was added to the *in vitro* cultures (blue histogram), PBS controls (red histograms). (e and f) 2P imaging of GAPs and LP-DCs in carbamylcholine (CCh) treated mice. Carbamylcholine (CCh) increased the number of GAPs and the co-localization of 10kD dextran (red) with LP-DCs (green). (f, Inset), LP-DCs capturing dextran (white arrowheads). (g) Luminal antigen presentation by LP-DCs following CCh administration as compared to controls given luminal Ova. (h) GF mice had increased GAPs (red = 10kD dextran; DAPI, blue). (i) Luminal antigen presentation by LP-DCs from GF mice was significantly enhanced compared to LP-DCs from SPF housed mice. CD103^{+} LP-DCs presented luminal antigen significantly better than CD103^{-} LP-DCs from GF mice. (j) 2P imaging of intestines in Math1$^{fl/flVilCre}$ mice (M1KO). M1KO mice lacked GAPs (red, 10 kD dextran) in the epithelium (blue, DAPI). (k) Luminal antigen presentation by LP-DCs from M1KO mice was undetectable. Scale bar in a = 20μm and f = 40μm. ns = not significant. * = $p<0.05$, ** = $p<0.01$, *** = $p<0.001$. Error bars = SEM. Data in d, g, and k are representative of three or more independent experiments, data in (i) was representative of two independent experiments. In (e), n = 15 or more images obtained from 3 animals for each condition.